Applied Field/Frequency Dependency of Propagation in Axially Magnetized Ferrite Waveguides

Bernice M. Dillon and Andrew A. P. Gibson

Abstract—**Vector finite element solvers are used to calculate phase constants and cutoff wave numbers in waveguides containing axially magnetized ferrite media. For phase constant calculations, ferrite characteristics are specified in terms of the applied field, frequency, and material characteristics including saturation magnetization and data from the hysteresis curve. Periodic boundary conditions are used with both finite element formulations to improve efficiency by reducing the size of the meshed region. Cutoff planes and phase shifts have been calculated for two examples, a Reggia–Spencer phase shifter and a ridged Faraday rotation section. In each case comparisons are made with measured data in the literature. The ridged Faraday section was found to be multimoded over the design bandwidth. For completeness, the geometrical dependency of the cutoff plane in circular quadruply ridged waveguides is enunciated and compared with available experimental results.**

Introduction

AXIALLY magnetized gyromagnetic waveguide structures are of ongoing interest as microwave phase shifter and control components. Cutoff planes and phase constants of regular axisymmetric cross sections are well understood and can be calculated analytically [1]. More complicated inhomogeneous waveguide cross sections require analysis using a numerical method. Finite elements are often chosen because of the ease with which arbitrarily shaped structures can be modeled. A number of different formulations have been proposed [2]–[4]. Troublesome spurious solutions in vector formulations can be now avoided and a number of remedies have recently been reviewed [5]. Another useful development is a formulation which allows the direct calculation of the modal phase constant rather than the wave number [6]. Recently this formulation has been applied successfully to axially magnetized axisymmetric waveguides [7]. In this paper, calculation of the modal characteristics for more practical inhomogeneous ferrite waveguide geometries is undertaken.

For design purposes, it is preferable to relate the waveguide characteristics to experimental material properties such as applied bias field and frequency rather than the entries of the tensor permeability (κ, μ). Analytical solutions of the characteristic equations and numerical calculations are commonly presented in terms of these tensor entries [1]–[4], [5], [7]. Although this approach suitably describes the properties of the waveguide it is difficult to relate results to measured data because of the frequency dependency of (κ, μ). An extension to the phase constant formulation is presented here to include specification of ferrite parameters in terms of experimental data. Formulas to relate magnetization, frequency, applied field, and material characteristics are chosen to include partially magnetized states [8]. Waveguide symmetry is used where possible to reduce the size of the meshed region and solves the geometry more efficiently [9]. Axially magnetized ferrite waveguides do not support conventional reflection symmetry so mirror planes cannot be used. However, these waveguides usually exhibit some rotational symmetry. In finite element analysis, rotational symmetry is modeled using periodic boundary conditions. These types of boundary constraints are often used in low-frequency analysis of electrical machines [11]; however their use in high-frequency work is uncommon. The periodic boundary constraints relate the tangential field components along two azimuthal planes of the waveguides. These boundary constraints can be used with both the wave number and the phase constant formulations.

Two examples from the literature are chosen to illustrate the usefulness of finite element analysis in practical device design. Reggia–Spencer phase shifters produce large phase shifts in a partially magnetized state [11]–[13]. In accordance with the suppressed-rotation theory of operation [12], the finite element calculations illustrate how one orthogonal mode is below cutoff, whereas the other is above and will propagate. Phase shift calculations with specified frequency and applied field agree with experimental behavior. Quadruply ridged circular waveguides containing ferrite rods are designed to give broadband Faraday rotation [14]–[16]. Phase shift calculations for these geometries agree with experimental results. Cutoff calculations show that care must be taken not to excite a higher order mode which is observed to have a cutoff close to that of the dominant operating mode. Results are also presented to illustrate the variation of the cutoff planes with ridge size in an empty quadruply ridged waveguide. These results agree with experimental results and also indicate that the higher-order mode in the quadruply ridged Faraday rotation section is related to one of the circularly polarized TE_{21} modes in a circular waveguide.

Manuscript received March 29, 1993; revised June 15, 1993. This work was supported by the Science and Research Council (England).

The authors are with the Department of Electrical Engineering and Electronics, UMIST, P.O. Box 88, Manchester M60 1QD, England.

IEEE Log Number 9212959.

Finite Element Analysis

The time-harmonic magnetic field within a waveguide containing gyromagnetic media satisfies the vector wave equation:

$$\nabla \times (\epsilon_r^{-1} \nabla \times \boldsymbol{H}) - k_0^2 \hat{\mu}_r \boldsymbol{H} = 0 \tag{1}$$

where k_0 is the wave number of free space. In the usual way, the waveguide is assumed to be uniform in the z direction, so all field components have a z-dependence of $e^{-j\beta z}$ where β is the phase constant. For inhomogeneous waveguides containing ferrite, both the scalar relative permittivity ϵ_r and the tensor relative permeability $\hat{\mu}_r$ are functions of position.

For design purposes, two types of calculations on a waveguide cross section are required to fully determine its modal characteristics: calculation of the modal hierarchy in the cutoff plane identifies all modes which may propagate at a particular frequency; calculation of the phase constant of the propagating modes at a specified frequency gives the dispersion associated with the mode. As described in [7] the finite element (FE) method can be used to solve both types of problems. The functionals used in each case are different but the solution procedure, including, for example, element assembly and imposition of boundary constraints, etc., is essentially the same. The cutoff plane can be calculated using the vector field functional first described by Berk [17] and since then widely used [5]. With this functional, the phase constant β is specified and the wave number is calculated as the eigenvalue. To evaluate the phase constants at a specified frequency, a functional in terms of transformed field components is used [6], [7]. The frequency is specified and the eigenvalues correspond to β^2. In both cases the eigenvectors correspond to the magnetic field of the modes.

Modeling Saturated and Partially Magnetized Ferrites

Analytical phase constant and cutoff plane calculations in ferrite waveguides are often presented in terms of the ratio of the off diagonal to main diagonal permeability tensor entries [1], [18]. This parameter is chosen for mathematical convenience. As it is a function of the frequency, applied field, and magnetization, it is not easy to relate the predicted characteristics to measured results. For waveguide design purposes, calculations in terms of either frequency or applied field are more useful and can be readily compared with measured data.

Most other finite element solvers for ferrite waveguides described in the literature are based on the wave number formulation. Both Konrad [2] and Wang and Ida [3] calculate resonant frequencies in axially magnetized cavities. Gibson and Helszajn [4] study the modal characteristics of elliptical ferrite waveguides. In each case, the tensor permeability used is of the form

$$\hat{\mu}_r = \begin{bmatrix} \mu & -j\kappa & 0 \\ j\kappa & \mu & 0 \\ 0 & 0 & \mu_{zz} \end{bmatrix} \tag{2}$$

where an axial bias field has been assumed. The values of the tensor components are specified and results are often presented in terms of κ/μ. The functional for the wave number cannot easily be extended to include the frequency dependence of the ferrite materials. As shown in the Appendix, the resulting matrix equation will not be a standard eigenvalue problem. Thus, for calculation of cutoff wave numbers, the ferrite is specified in terms of κ and μ as given in (2).

Compared with wave number formulations, finite element functionals with eigen-phase solutions have one additional advantage (exploited here), that ferrite characteristics can be incorporated into the formulation. By specifying the ferrite characteristics in terms of a set of experimental parameters, the value of the tensor components for a signal frequency and applied field can be calculated. The complicated magnetic behavior of ferrites, especially if partially magnetized, means that a full theoretical model is not available [19]. For saturated ferrites, the relationship between the tensor entries and the material characteristics is well-known [1], [18], [19]. The value of the magnetization is known and for any applied field and frequency the tensor components can be calculated. Difficulties arise for partially magnetized ferrites where the value of the magnetization for a particular applied field is not known. A set of formulas suitable for all magnetizations higher than the remanence level, have been proposed by Hansson and Filipsson [8]. The values of the tensor components in (2) are given as [8]:

$$\begin{aligned} \mu_{zz} &= \mu_0^{1-p^{5/2}} \\ \mu &= \mu_0 + (1 - \mu_0)p^{3/2} + \frac{\eta^2 H_0 M}{(\eta H_0)^2 - \omega^2} \\ \kappa &= \frac{\omega \eta M}{(\eta H_0)^2 - \omega^2} \end{aligned} \tag{3}$$

where ω is the frequency of operation, H_0 is the internal field and η is the gyromagnetic ratio. The variable p is the ratio of the magnetization M to the saturation magnetization M_s [8]:

$$p = \frac{M}{M_s} = a_1 + (1 - a_1)\left\{ \coth (a_2 H_0) - \frac{1}{a_2 H_0} \right\} \tag{4}$$

where a_1 and a_2 are constants derived from the hysteresis curve of the material—a_1 is equal to the ratio of the remanent and saturation magnetizations and a_2 is related to the slope of $dB/dH|_{H=0}$. In (4), μ_0 is the scalar permeability in the demagnetized state

$$\mu_0 = \frac{1}{3} + \frac{2}{3}\sqrt{1 - \frac{(\eta M)^2}{\omega^2}} \tag{5}$$

where the effects of the anisotropy field have been neglected. The values predicted by these formulas agree reasonably well with measured data for a range of ferrites [8]. These formulas have been incorporated into the FE phase constant solver so that the ferrite is specified in

terms of material characteristics, an applied field, and a frequency. Comparisons can then be easily made between measured and calculated results.

Periodic Boundary Conditions

Vector finite element solutions of waveguide cross sections is a computationally expensive procedure. Reductions in the size of the meshed region of the waveguide cross section can lead to significant savings in computer time. In waveguide geometries with materials characterized by scalar material properties, mirror planes of symmetry are used to reduce the size of the meshed region [9]. The mirror planes are modeled as electric or magnetic walls. Waveguides with axially magnetized ferrite media do not support mirror symmetry. The bias magnetic field along the direction of propagation is an axial vector and hence it is never mapped onto itself by a reflection in the transverse plane of the waveguide. However, these waveguides can support rotational symmetry: both the waveguide geometry and the bias field can be mapped onto themselves by a rotation of a fractional part of 360°.

Rotational symmetry can be used to relate the vector field components along two azimuthal planes in the waveguide to each other

$$\boldsymbol{H}(r, \theta) = \boldsymbol{m} \cdot \boldsymbol{H}(r, \theta + \phi) \tag{6}$$

where ϕ is the angle of rotation. The matrix $\boldsymbol{m}$ is a 3×3 matrix whose values are defined by the symmetry of the required modal solution. In general, for a waveguide with rotational symmetry of $\phi = 360/n$, each of its modes will exhibit one of n possible symmetries. Thus, to calculate all the modes, there are n sets of rotational boundary conditions which constrain the tangential field components along the azimuthal planes on the section ϕ of the waveguide. Each set of rotational boundary conditions has a unique $\boldsymbol{m}$ matrix in (6). A systematic procedure for calculating the components of the matrix uses the fact that after n rotations each mode is mapped onto itself. The matrix $\boldsymbol{m}$ is given as

$$\boldsymbol{m} = \alpha_i \begin{bmatrix} \cos\phi & \sin\phi & 0 \\ -\sin\phi & \cos\phi & 0 \\ 0 & 0 & 1 \end{bmatrix} \tag{7}$$

where α_i is one of the nth roots of unity and the matrix on the right-hand side is the standard transformation matrix for a rotation of an angle ϕ. For $n = 2$, the corresponding $\alpha = \{1, -1\}$ and for the case of $n = 4$, $\alpha = \{i, -i, 1, -1\}$.

Equations (6) and (7) are used to specify the relationship between the tangential field components of the modes along the azimuthal planes of the waveguide. This relationship can be incorporated into either FE formulation as a periodic boundary condition. These types of boundary conditions do not alter the symmetry of the matrix nor do they involve evaluating any line integrals over the mesh boundaries. Periodic boundary conditions have not been widely used in waveguide analysis. One reason is that for rotational symmetry with $n > 2$, the components of the matrix $\boldsymbol{m}$ in (6) are often complex. Thus, even waveguides containing scalar lossless media generate a complex matrix equation. For these geometries it is more efficient to use reflection symmetry to reduce the size of the mesh because the matrices involved remain real. With ferrite media however, the matrices are complex in any case and so the use of periodic boundary conditions to reduce the size of the mesh is appropriate.

Reggia–Spencer Phase Shifter

Rectangular waveguides with a centrally positioned ferrite rod are used as variable phase shifters. This type of phase shifter, first proposed by Reggia and Spencer [11], usually operates at low applied dc fields where the differential phase shift varies rapidly with applied dc field. A typical geometry is illustrated in Fig. 1. Only rotational symmetry can be used to reduce the size of the mesh because of the axially magnetized ferrite rod. This means that half the structure must be modeled instead of a quarter which could be used with mirror planes if the structure contained scalar media only. About 20 covariant-projection elements [20] were used to construct the mesh for the following calculations.

Cutoff Planes Calculations

Fig. 2 shows the cutoff plane variation of the dominant mode and the cross-polarized higher order mode with the size of the ferrite rod. Hord, Rosenbaum, and Boyd [12] proposed a theory of suppressed rotation to explain the mechanism of phase shifting. According to this theory, the large phase shifts are due to tensor-induced coupling between the dominant mode and a cross-polarized evanescent mode. The TE_{10} dominant linear-polarized mode in an empty rectangular waveguide will propagate as an elliptically polarized hybrid HE_{10} mode in the ferrite-loaded waveguide. From Fig. 2, the optimum width of ferrite can be chosen for any required frequency of operation. For large phase shifts, the rod size is ideally constrained so that the cross-polarized mode is just below cutoff [11]–[13].

Phase Constant Calculations

A comparison between measured phase shift results and FE calculations are shown in Fig. 3. These results illustrate the increased phase shift associated with a larger ferrite rod when the cross-polarized mode is close to cutoff. The coupled mode results [12], achieved using a ferrite slab in the waveguide, are shown for comparison. In the FE calculations each mesh was solved twice at each frequency; once with zero applied field and next with a small applied field. The modal field plot in Fig. 4 illustrates the concentration of the dominant mode in the ferrite region. Calculations for the variation in phase shift with applied field for different sized ferrites are shown in Fig. 5. The dramatic change in phase shift for different sized ferrites

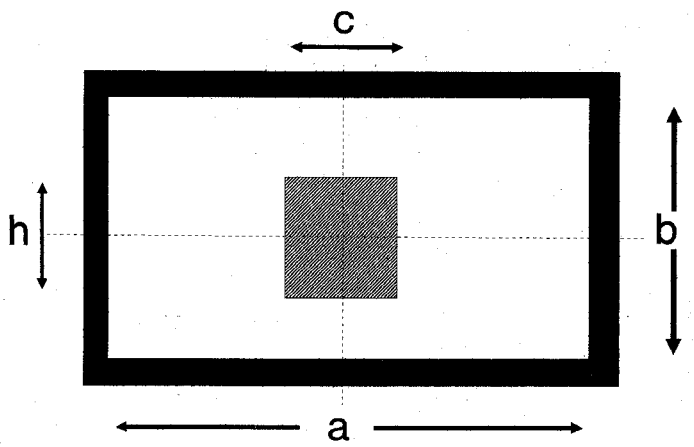

Fig. 1. Schematic geometry of Reggia–Spencer phase shifter cross section. $b/a = 0.444$, $h/a = 0.222$. Waveguide is air-filled except for hatched region which is ferrite: $k_m a = 2.9$, $\epsilon_f = 13$.

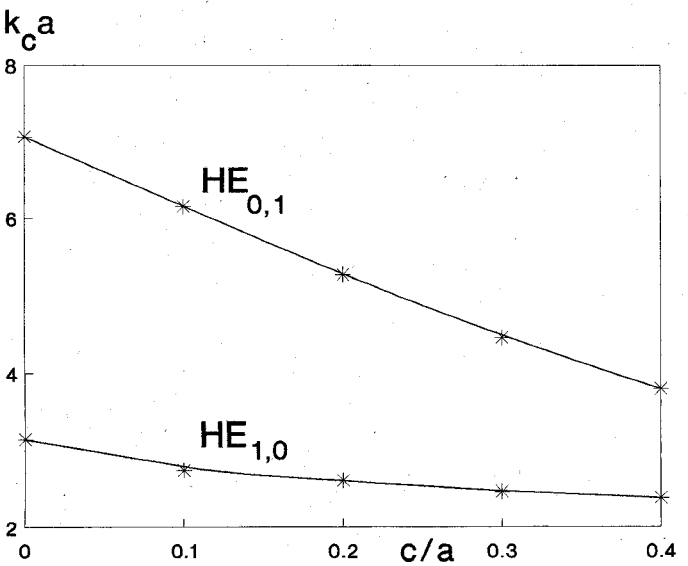

Fig. 2. FE calculations for the cutoff plane of the dominant and orthogonal mode. The geometry is as shown in Fig. 1.

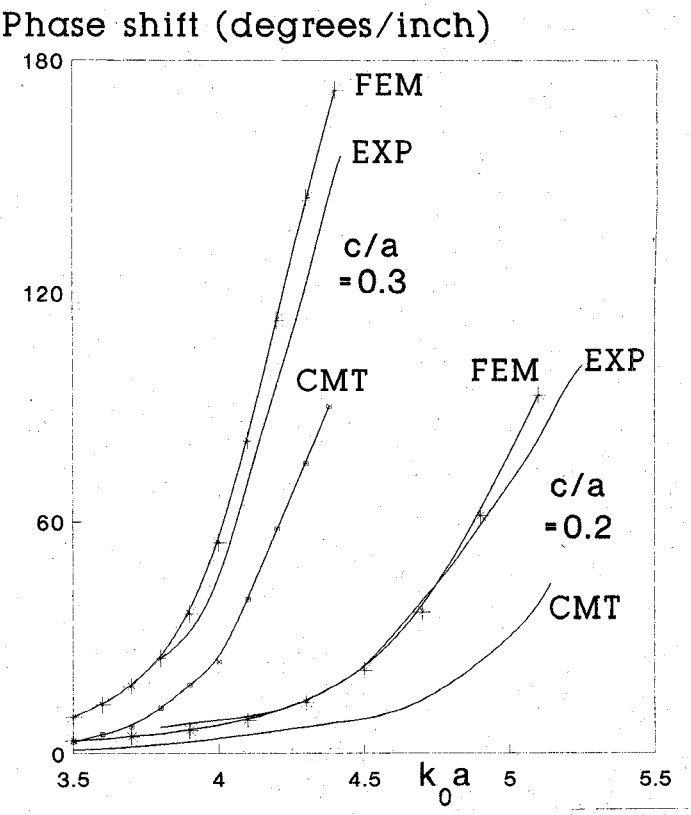

Fig. 3. Variation in differential phase shift with frequency. The coupled mode (CMT) results were calculated for $b/h = 1$. The finite element method (FEM) results were obtained using the geometry in Fig. 1 with $H_{dc} = 0.0$ and $H_{dc} = 1$ Oe. Both the coupled mode and measured data [EXP] are from [12].

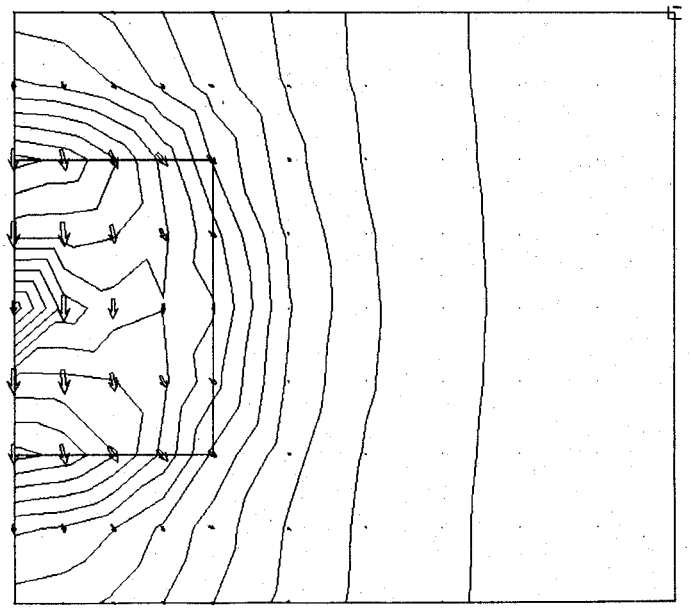

Fig. 4. Transverse magnetic field for the dominant elliptically polarized HE_{10} mode. $H_{dc} = 10$ Oe, $k_0 a = 4.4$. Half the geometry in Fig. 1 was meshed.

is typical of this class of phase shifters [11]–[13]. For low values of the applied field, the FE results may not correlate exactly with experimental values because of the limitations of the model used to characterize the ferrite [8]. However, the results in Figs. 3 and 5 indicate that the FE solver models the behavior of these partially magnetized phase shifters reasonably well.

Quadruply Ridged Faraday Rotation Section

Faraday rotation sections may be constructed using an axially magnetized ferrite rod centrally positioned in a circular waveguide. When the ferrite is magnetized, the circular polarized modes in the waveguide travel at different phase velocities. For wide-band applications, a nearly constant rotation with frequency is required. One way of achieving this is to lower the cutoff frequency of the propagating mode, thereby reducing the effect of dispersion. A typical quadruply ridged Faraday rotation cross section is illustrated in Fig. 6. This type of geometry has been proposed by Chait and Sakiotis [14] among others, to improve the bandwidth characteristics of Faraday rotator sections.

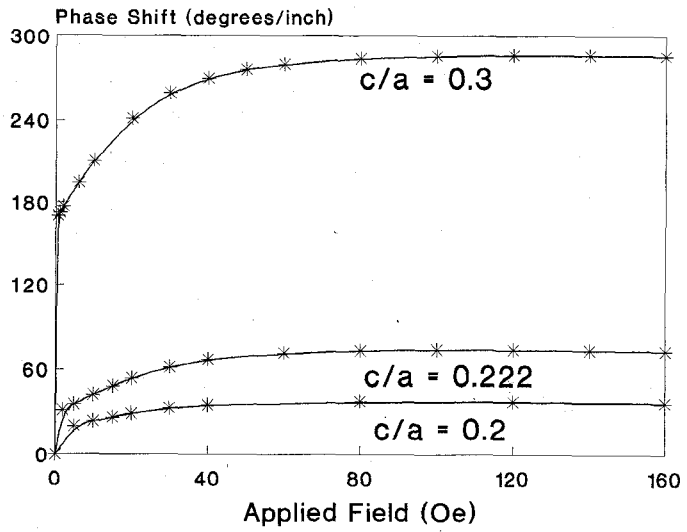

Fig. 5. Finite element calculations for the variation in differential phase shift with applied dc magnetic field for different ferrite widths. $k_0a = 4.4$.

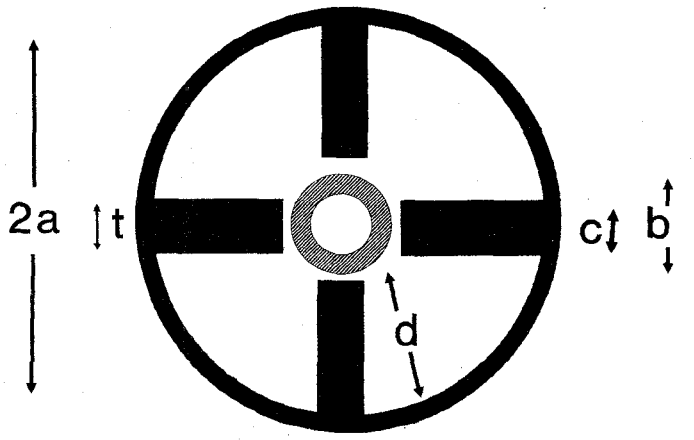

Fig. 6. Schematic geometry of quadruply ridged Faraday rotator. a = 11.944 mm, b = 6.426 mm, $c = t$ = 3.175 mm. Waveguide is air-filled except for hatched region which is TT-390 ferrite: M_s = 2150 G, H_{dc} = 384 Oe, and ϵ_f = 12.7.

Cutoff Plane Calculations

The cutoff wave numbers of a quadruply ridged circular waveguide with an axially magnetized ferrite rod (Fig. 6) were evaluated. These calculations were done over a quarter section of the guide using a mesh of about 20 covariant projection elements with rotational boundary conditions. Cutoff plane calculations for an axisymmetric ferrite waveguide and a quadruply ridged ferrite waveguide are shown in Fig. 7. In general, the ridges lower the cutoff wave numbers of the HE_{mn} modes and increase the cutoffs of the EH_{mn} modes. This is similar to the behavior of the corresponding modes in the empty ridge case as described in the next section. For axisymmetric structures, Waldron [1] has shown that the cutoffs of the HE modes is unaffected by the magnetization (κ/μ) whereas the cutoffs of the EH modes split. FE calculations indicate that the introduction of the ridges does not affect this behavior. It is also worth noting that the ferrite-loaded ridged waveguide supports an HE_{21} mode close in cutoff to the dominant

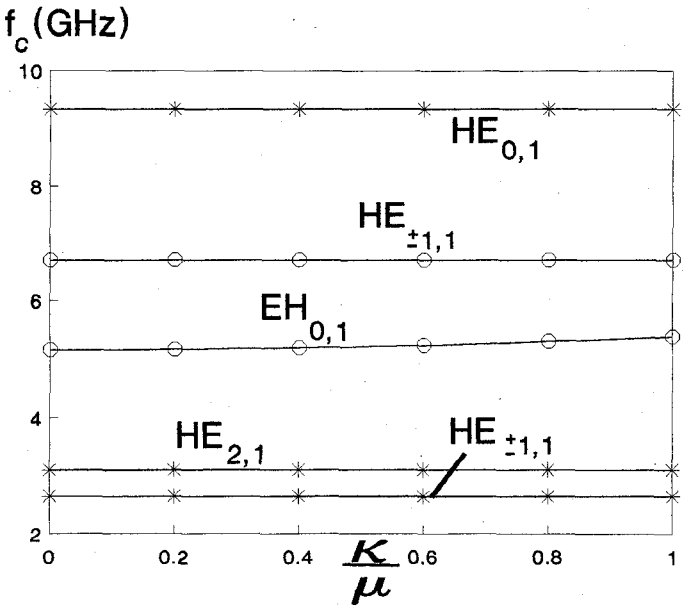

Fig. 7. FE calculations for the cutoff wave numbers in the Faraday rotation section with d/a = 0.0 [—O—] and with d/a = 0.73 (—*—).

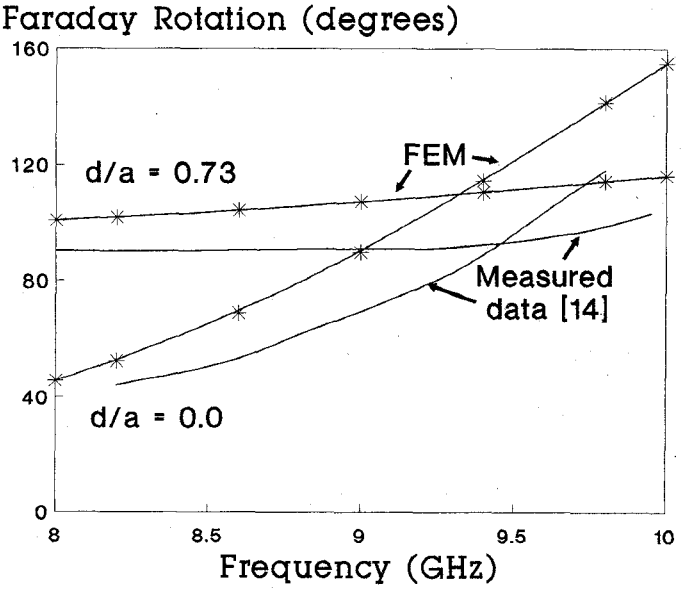

Fig. 8. Faraday rotation for a circular waveguide, with and without ridges. The length of the guide is 50.8 mm.

pair of modes. The quadruply ridged Faraday rotation section are therefore multimoded over the proposed bandwidth of 8–9.6 GHz.

Phase Constant Calculations

The Faraday rotation in a given length of ferrite can be calculated by evaluating the differential phase constants of the dominant $HE_{\pm 1,1}$ circularly polarized modes. Identical meshes and boundary conditions to those used with the cutoff plane calculations were employed for evaluation of the phase constants. Each mesh was solved twice to obtain the positive and negative circularly polarized modes. Fig. 8 shows the calculated phase shift of the Faraday rotator section in Fig. 6, with and without ridges.

There is a significant improvement in the bandwidth when the ridges are in place. Measured data for the improvement in a 90° rotator based on a similar geometry described in [14] is also shown in Fig. 8 for comparison. The reduced phase shift in the measured results may be due to dielectric loading which was possibly used together with the ridges to enhance the bandwidth characteristics of the rotator. In addition, the ferrite rod is often tapered at both ends to improve matching. No allowance was made for this in the finite element calculations where a uniform rod was assumed.

Cutoff Planes of Empty Quadruply Ridged Waveguides

In the design of the rotator, Chait and Sakiotis experimentally investigated the effect of ridges on the cutoff wave number of the dominant mode in an empty circular waveguide. These measured results were used to check the accuracy of the FE cutoff wave number calculations and good agreement was found as shown in Fig. 9. To examine the modal hierarchy of these waveguides in more detail, the geometrical dependence of the cutoffs of the first few modes was studied. Ridge length was found to have a more significant effect than ridge thickness. Fig. 10 shows the variation in cutoff frequency with ridge length for four infinitely thin ridges. These calculations were done by modeling one quarter of the waveguide geometry using up to 40 covariant projection elements. Reflection symmetry was used to specify the boundary conditions and so there were three sets of modal solutions: two magnetic walls (MM), magnetic and electric walls (ME), and two electric walls (EE). In Fig. 9 the modes are labeled according to their nomenclature in a circular waveguide. The mode nomenclature for circular guides assumes degeneracy between clockwise and anticlockwise mn modes ($m > 0$). The presence of the ridges upsets the degeneracy in pairs of TE and TM modes which do not satisfy the mixed ME boundary conditions on a quarter section. In Fig. 9 one of the TE_{21} modes satisfies the EE boundary condition and so is unaffected; however, the cutoff of the other TE_{21} mode which satisfies the MM boundary conditions tends towards zero as the ridges increase in length. In general, the ridges increase the cutoff values of the TM modes and decrease those of the TE modes which do not satisfy the EE boundary condition. These calculations show that the cutoff of the dominant pair of modes is substantially reduced for fairly long ridges $d/a > 0.6$ with moderate thickness. This agrees with the conclusions reached in [14]. Chait and Sakiotis [14] do not investigate the effect of the ridges on the cutoffs of any other mode apart from the dominant mode. Rong *et al.* [16] use a combined boundary element and mode expansion method to calculate the modes in similar waveguides. They provide data for the cutoffs of both the dominant TE_{11} modes and the TM_{11} modes only. Note that Fig. 10 shows that the cutoff of one of the circularly polarized TE_{21} modes is reduced significantly by the ridges.

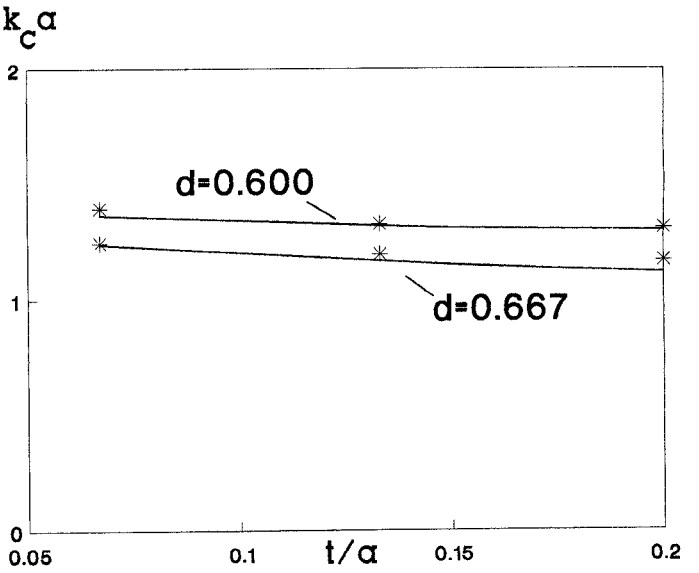

Fig. 9. Comparison between calculated finite element [*] results and measurements [14] for the variation in cutoff of the dominant $TE_{\pm 1,1}$ modes with ridge thickness.

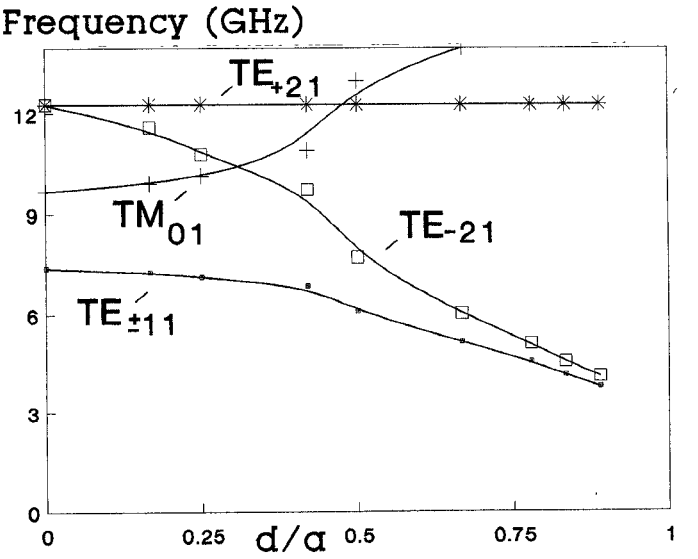

Fig. 10. FE calculations for the variation of the modal cutoff wave numbers with length of ridges. $t = 0$.

Conclusions

Finite element methods have been used to evaluate the modal characteristics of practical inhomogeneous axially magnetized ferrite waveguides. A complete description of the two functionals and the FE solution schemes used here can be found in [7]. Two aspects of the formulation which have been extended to allow easier modeling of practical geometries are described. Ferrite materials are characterized in the phase constant formulation using standard material data, the applied bias field, and the frequency. The formulas used to relate magnetization, frequency, applied field, and material characteristics allow modeling of the partially magnetized states so long as the applied bias field is above remanence. Secondly, rotational symmetry is used to define appropriate periodic boundary conditions

for the calculation of the waveguide modes on a section of the waveguide. This means results for general non-axisymmetric axially magnetized waveguides can be calculated more efficiently. Cutoff planes, phase constants, and modal field patterns can be calculated. Results from two typical waveguide cross sections—a quadruply ridged Faraday rotation section and a Reggia–Spencer phase shifter are described.

Appendix

The functional for the calculation of the cutoff wave number is

$$F(\boldsymbol{H}) = \int_S \{\epsilon_f^{-1}|\nabla_t \times \boldsymbol{H}_t|^2 - k_0^2 [\boldsymbol{H}_t^* \cdot \hat{\mu}_{tt}\boldsymbol{H}_t + H_z^* \mu_{zz} H_z] + \epsilon_f^{-1}|\nabla_t H_z + j\beta \boldsymbol{H}_t|^2\}\, dS \quad \text{(A.1)}$$

where S is the cross section of the waveguide, * denotes complex conjugate, and the phase constant β is specified. Both the magnetic field $\boldsymbol{H}$ and the tensor permeability have been split into a transverse and axial part in (A.1). Assuming a tensor of the form given in (2), the second term in the integrand of (A.1) becomes

$$k_0^2 [\boldsymbol{H}_t^* \cdot \hat{\mu}_{tt}\boldsymbol{H}_t + H_z^* \mu_{zz} H_z] = \omega^2 \mu_0 \epsilon_0 [H_z^* \mu_{zz} H_z + \mu(H_x^* H_x + H_y^* H_y) + j\kappa(H_y^* H_x - H_x^* H_y)] \quad \text{(A.2)}$$

where ω is the unknown frequency of operation. In ferrites which are saturated, the relationship between the tensor entries and the material characteristics is well-known [1]:

$$\mu = 1 + \frac{\omega_0 \eta M_s}{\omega_0^2 - \omega^2}, \qquad \mu_{zz} = 1 \quad \text{(A.3a)}$$

$$\kappa = \frac{\omega \eta M_s}{\omega_0^2 - \omega^2} \quad \text{(A.3b)}$$

where w is the frequency of operation, $\omega_0 = \eta H_0$, M_s is the saturation magnetization, H_0 is the dc applied field, and η is the gyromagnetic ratio. Substitution for κ and μ in (A.2) gives a final integrand involving terms with ratios of $\omega^2/(\omega_0^2 - \omega^2)$, $\omega^3/(\omega_0^2 - \omega^2)$ as well as terms with ω^2. The corresponding matrix equation cannot be easily solved for ω using standard eigenvalue matrix routines.

Acknowledgment

The authors thank GEC–Marconi, Stafford, for the use of their finite element pre- and post-processing package SLIM.

References

[1] R. A. Waldron, "Electromagnetic wave propagation in cylindrical waveguides containing gyromagnetic media," *J. Brit. Instn. Radio Engnrs.*, vol. 18, pp. 597, 677, 733, 1958.

[2] A. Konrad, "Vector variational formulation of electromagnetic fields in anisotropic media," *IEEE Trans. Microwave Theory Tech.*, vol. MTT-24, pp. 553–559, Sept. 1976.

[3] J. Wang and N. Ida, "Eigenvalue analysis in anisotropically loaded electromagnetic cavities using edge finite elements," *IEEE Trans. Magnetics*, vol. 28, pp. 1438–1441, Mar. 1992.

[4] A. A. P. Gibson and J. Helszajn, "Finite element solution of longitudinally magnetized elliptical gyromagnetic waveguides," *IEEE Trans. Microwave Theory Tech.*, vol. 37, pp. 999–1005, June 1989.

[5] B. M. Rahman, F. A. Fernandez and J. B. Davies, "Review of finite element methods for microwave and optical waveguides," *Proc. IEE*, vol. 79, pp. 1442–1448, Oct 1991.

[6] J. Lee, D. Sun and Z. J. Cendes, "Full-wave analysis of dielectric waveguides using tangential vector finite elements," *IEEE Trans. Microwave Theory Tech.*, vol. 39, pp. 1262–1271, Aug. 1991.

[7] B. M. Dillon, A. A. P. Gibson and J. P. Webb, "Cut-off and phase constants of partially filled, axially magnetized, gyromagnetic waveguides using finite elements," *IEEE Trans. Microwave Theory Tech.*, vol. MTT-41, May 1993.

[8] B. Hansson and G. Filipsson, "Microwave circulators in stripline and microstrip techniques," Tech. Rep. No. TR 7606, Chalmers University of Technology, Gothenburg, Sweden, June 1976.

[9] P. P. Silvester and R. L. Ferrari, *Finite Elements for Electrical Engineers*. Cambridge, MA: Cambridge University Press, 1990.

[10] H. Hoole and S. Ratnajeevan, *Computer-Aided Analysis and Design of Electromagnetic Devices*. New York: Elsevier, 1989.

[11] F. Reggia and E. G. Spencer, "A new technique in ferrite phase shifting for beam scanning microwave antennas," *Proc. IRE*, vol. 45, pp. 1510–1517, Nov. 1957.

[12] W. E. Hord, F. J. Rosenbaum and C. R. Boyd, "Theory of the suppressed-rotation reciprocal ferrite phase shifter," *IEEE Trans. Microwave Theory Tech.*, vol. MTT-16, pp. 902–910, Nov. 1968.

[13] J. A. Weiss, "A phenomenological theory of Reggia–Spencer phase shifter," *Proc. IRE*, vol. 47, pp. 1130–1137, June 1959.

[14] H. N. Chait and N. G. Sakiotis, "Broad-band ferrite rotators using quadruply ridged circular waveguides," *IRE Trans. Microwave Theory Tech.*, vol. MTT-7, pp. 38–41, Jan. 1959.

[15] E. S. Grimes, D. D. Bartholomew, D. C. Scott and S. C. Sloan, "Broad-band ridge waveguide ferrite devices," *IRE Trans. Microwave Theory Tech.*, vol. MTT-8, pp. 489–492, 1960.

[16] Y. Rong, W.-B. Dou and S. F. Li, "Generalised field theory of irregular waveguides partially filled with longitudinally magnetized ferrite," *IEE Proc.-H*, vol. 138, no. 5, pp. 412–416, Oct. 1991.

[17] A. D. Berk, "Variational principles for electromagnetic resonators and waveguides," *IRE Trans. Antennas Propagat.*, vol. AP-4, pp. 104–111, Apr. 1956.

[18] J. Helszajn, *Ferrite Phase Shifters and Control Devices*. New York: McGraw-Hill, England, 1989.

[19] R. F. Sooho, *Microwave Magnetics*. New York: Harper & Row, 1985.

[20] R. Minowitz and J. P. Webb, "Covariant-projection quadrilateral elements for the analysis of waveguides with sharp edges," *IEEE Trans. Microwave Theory Tech.*, vol. 39, pp. 501–505, Mar. 1991.

Bernice M. Dillon received the B.A.I. degree in Engineering from Trinity College, Dublin, Ireland in 1984. From 1984 to 1986 she worked as a design engineer for Mentec Ltd., Dublin. She received a Ph.D. from Cambridge University, England in 1990. Currently she is working as an SERC post-doctoral Fellow in the Dept. of Electrical Engineering and Electronics at UMIST.

Andrew A. P. Gibson was born in Dunfermline, Scotland in 1962. In 1985 he was awarded the Institution Prize from the IEE for distinction in obtaining the M.Eng. degree in Electrical and Electronic Engineering from Heriot-Watt University, Edinburgh, Scotland. In 1988 he received the Ph.D. degree from Heriot-Watt University after completing research into the finite element analysis of gyromagnetic waveguides. Currently, Dr. Gibson lectures at UMIST.